Mechanism of Dihydrogen Formation in the Magnesium–Water Reaction[⊥]

Irwin A. Taub,[†] Warren Roberts,[‡] Sebastian LaGambina,[§] and Kenneth Kustin*[,‖]

U.S. Army Natick Soldier Center, Natick, Massachusetts 01760-5018, Somerville High School, Somerville, Massachusetts 02143, and Department of Chemistry Emeritus, Brandeis University, P.O. Box 9110, Waltham, Massachusetts 02454-9110

Received: November 30, 2001; In Final Form: June 17, 2002

The thermodynamically favored reaction between water and magnesium, $Mg + 2H_2O \rightarrow Mg(OH)_2 + H_2$, is normally sluggish, but it becomes reasonably rapid when a milled composite of powdered magnesium metal and powdered iron (1–10 mol %) is used with sodium chloride solutions. Iron functions as an activator, and chloride functions as a catalyst that depassivates the outermost oxide/hydroxide layer and allows water to penetrate to the activated magnesium surface. Adding solutes such as sodium nitrate, copper(II) chloride, and sodium trichloroacetate to the reaction mixture suppresses the yield of dihydrogen. Manometric and calorimetric studies on the stoichiometry and kinetics of the reaction between Mg(Fe) powders and aqueous solutions demonstrate that short-lived, partially, and fully solvated electrons (e_p^- and e_s^-) are precursors of dihydrogen and that they and the hydrogen atoms ($H^•$) formed from them can be scavenged, resulting in suppressed dihydrogen yields.

Introduction

Because magnesium metal is useful metallurgically[1] and chemically,[2] the reaction of magnesium with water is extremely important. It is the process responsible for the corrosion of the magnesium, which limits the metal's metallurgical uses, except when corrosion is deliberately allowed, as in galvanic protection.[3] In contrast to metallurgical applications where the magnesium–water reaction is most often regarded as a nuisance, it is useful in chemical applications, for example, to generate heat or dihydrogen. With magnesium so widespread, the magnesium–water reaction should have been intensively studied, but the reaction is poorly described, except to emphasize its slowness.[4]

The sluggishness of the magnesium–water reaction, despite its accompanying favorable free energy change, is due to passivation of the metal by an unreactive oxide/hydroxide layer on the surface.[3] Anions presumed to be unreactive, particularly chloride, are often added as catalysts to speed up the reaction,[5] because they destroy the oxide/hydroxide layer's integrity. Even this anionic catalysis of the reaction is often insufficient for practical use, so it is further accelerated by using the metal milled with a small amount of iron (usually 5 mol %).[6]

We have found that this acceleration is not due to catalysis, since a very small amount of iron is consumed in the reaction and the extent of interfacial contact between Mg and Fe is important. Moreover, the yield of dihydrogen can be reduced by simple inorganic and organic reagents, known from radiation chemical studies to be scavengers of the solvated electron (e_s^-) and the hydrogen atom ($H^•$). (Though the solvated electron in water is designated as e_{aq}^-, reflecting its aquation, a more general designation, e_s^-, is used here.) In this paper we show that studies of the kinetics of scavenging lead to a plausible mechanism for the magnesium–water reaction, with implications for corrosion control and wider technological applications.

Experimental Section

Materials. Identical results were obtained with Mg–Fe preparations from different vendors; one vendor's product was selected for these studies. Thus, reactive Mg particles containing 5 mol % Fe were obtained from Dymatron Corp., Lexington, KY, and were used without further treatment. These particles were characterized by scanning electron microscopy (SEM) and electron dispersive spectrometry (EDS) as being approximately 250 μm oblate spheres of Mg with smaller-sized Fe spheres embedded on their surface and in the interior. Solutions were made in water purified by a two-stage Millipore Corp. apparatus consisting of a Milli-RO 60 input and a Milli-Q reagent grade activated carbon, reverse osmosis output. Reagent grade chemicals were used throughout without further purification, unless otherwise noted: benzoic acid, copper(II) chloride dihydrate, maleic acid, pyruvic acid (sodium salt), sodium persulfate, and trichloroacetic acid (sodium salt) from Aldrich; sodium nitrate and sodium nitrite from Fisher; sodium chloride from Mallinckrodt; and chloroacetic acid from Sigma. Iron chelators α,α′-dipyridyl and 1,10-phenanthroline were from Eastman.

Methods. *Gas Chromatography.* Hydrogen as the sole gaseous product formed in the reaction of magnesium with water both in the absence and presence of scavengers was verified using a Hewlett-Packard Model 5890 Series II gas chromatograph. The gaseous atmosphere above the solution was sampled using a 25 mL gas-tight syringe and then injected into the chromatograph for separation and detection. An 80/100 mesh 5 Å molecular sieve hand packed into an 8 in. by 1/8 in. stainless steel column and maintained at 25 °C in an oven served to separate the N_2, O_2, and H_2. The column was preconditioned using multiple injections of a standard H_2 in N_2 mixture. Helium was used as the carrier gas and the flow rate was controlled at

* Author to whom correspondence should be addressed. E-mail: kmkustin@ix.netcom.com.
† U.S. Army Natick Soldier Center, Deceased.
‡ U.S. Army Natick Soldier Center.
§ Somerville High School.
‖ Brandeis University.
⊥ Dedicated to the memory of Dr. Irwin A. Taub.

10.1021/jp0143847 CCC: $22.00
Published on Web 08/03/2002

5 mL/min. A thermal conductivity detector maintained at 50 °C was used for monitoring the eluted gases and gave a negative signal for H_2 in the He. The proportion of H_2 in each sample was quantified using the Hewlett-Packard Chemstation software, based on peak area and calibrating H_2/N_2 standards.

Manometry. Gas volume measurements were made at timed intervals after adding preweighed samples of 5 mol % Fe-activated magnesium particles to the solutions. The gas formed changed the fluid level in a U-tube manometer fabricated from two 50 mL burets to which was attached at the bottom a flexible tubing that connected to a height-adjustable displacement fluid reservoir. One buret was connected to the reaction flask; the other was open to the atmosphere. Corrections to the volume of gas formed were made for standard pressure and temperature, for initial air inclusion, and for samples that differed from a 0.100 g standard, to which all measurements were scaled.

Calorimetry. The time course of the heat generated in the reaction was automatically monitored using a Parr Model 1455 Solution Calorimeter with a Model 1670 Controller. The time−temperature data were logged into a computer using instrumentation software such as Lotus Measure. The instrument time code was converted to elapsed time in seconds using a macro. Rate constants and other kinetics parameters were obtained from these curves by nonlinear exponential curve-fitting.[7] The Parr calorimeter used employs a stirrer. However, no differences were found between stirred and unstirred reaction solutions, because unstirred solutions are agitated by copious evolution of bubbles.

Results and Discussion

Iron-Activated, Chloride-Catalyzed, Magnesium−Water Reaction. Though ordinarily very slow, the thermodynamically favorable reaction of magnesium with water takes place reasonably fast if iron is in contact with magnesium and chloride ion is present. Superficial contact between the two metals leads to activation at the contact point only. Using powdered magnesium milled with smaller amounts of powdered iron ensures smooth and reproducible kinetics of heat and dihydrogen evolution. The rate of evolution increases with increasing iron, but beyond about 7−8 mol % Fe no further acceleration is observed; 5 mol % Fe was used in these studies. Typically, the reaction in a 2 M sodium chloride solution was complete within 30 min at which time the gas evolution ceased, all the magnesium was consumed, and a black magnetic powder remained on the bottom of the reaction flask.

To determine whether the iron acts as a catalyst or an activator of the reaction, we carried out spectrophotometric tests on the spent reaction solution. Since iron(II) salts dissolved in solution react with specific chelating agents to give intensely colored complexes even in the presence of iron(III) salts,[8] aliquots of the spent solution were removed and the chelators α,α′-dipyridyl and 1,10-phenanthroline were added to them. No evidence for formation of iron(II) on the basis of these tests was found. Since traces of $[FeCl(H_2O)_5]^{2+}$ should be directly observable at 336.2 nm in the presence of 2 M chloride ion, aliquots were scanned spectrophotometrically. The scans showed that a small amount of the elemental iron in the milled composite had oxidized to iron(III). From absorbance measurements, we determined that about 0.01% of the available iron in the milled mixture had reacted. Although activation is achieved without appreciable net change in the valence of the iron, it is possible that the small amount of observed chemical change plays some role in the reaction mechanism. To understand how iron might activate magnesium so that it reacts with water at a significant rate, some characteristics of the chloride ion-catalyzed reaction are first considered.

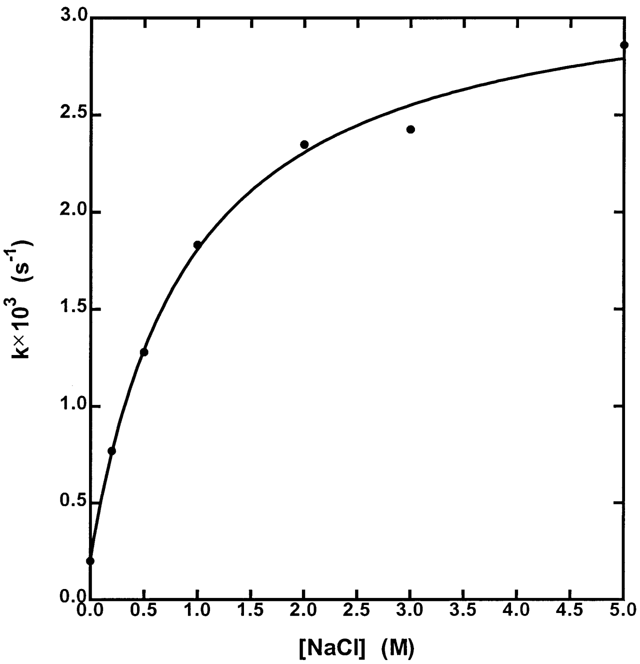

Figure 1. Chloride ion concentration dependence of the first-order rate constant for reaction between 5 mol % Fe-activated magnesium and water. Each experimentally observed rate constant, *k*, at a given chloride ion concentration (●) is an average of at least three calorimetric determinations of temperature evolution as a function of time at 25 °C. (For parameters of calculated curve see text.)

In the presence of chloride ion, the reaction between iron-activated magnesium and water is first-order in magnesium mass. Chloride ion catalysis increases with increasing chloride ion concentration, but saturates at about 3 M chloride ion concentration, the experimentally determined rate constant, *k*, changing only slightly thereafter (Figure 1). The rate constant was fitted to the function $k = k_o + (k_c K[Cl^-])/(1 + K[Cl^-])$, where k_o corresponds to the rate constant without chloride ion, k_c to the rate constant in the presence of chloride ion, and K to a binding constant. The values of these rate and binding constants are: $k_o = 0.20 \pm 0.069 \times 10^{-3}$ s^{-1}, $k_c = 3.05 \pm 0.08 \times 10^{-3}$ M^{-1} s^{-1}, and $K = 1.1 \pm 0.15$ M^{-1}.

If the entire powdered magnesium sample is in good contact with iron and in the presence of sufficient chloride ion, the reaction stoichiometry should be

$$Mg(s) + 2H_2O(l) \rightarrow Mg(OH)_2(s) + H_2(g) \qquad (1)$$

The reaction is accompanied by the release of a substantial amount of energy, 352.96 kJ mol^{-1} at 25 °C. For a 0.100 g sample of powdered magnesium with 5 mol % Fe, 89.8 mL of H_2 should be produced at 1 atm pressure and 25 °C. In a representative experiment using 0.05 g of sample to stay within the limits of the buret, 44.5 mL of H_2 was measured, consistent with the stoichiometry of reaction 1.

After the reaction is completed, the gaseous portion of the reaction chamber should contain H_2 and atmospheric gases. To verify that the increase in volume was due exclusively to H_2, three gaseous samples were collected from each of two reaction quantities of 0.0502 and 0.2492 g of 5 mol % Fe-activated magnesium with 2 M NaCl and then analyzed by gas chromatography. The only nonatmospheric gas detected was H_2. From the percentages of H_2, N_2, and O_2 in samples with differing proportions of evolved gases and from the ratio of N_2/O_2 being constant at 3.73 ± 0.53, it was concluded that only H_2 is produced and that no O_2 is consumed.

We assume that the thermodynamically favored reaction between magnesium and water at or close to neutrality is slow due to passivation by the oxides/hydroxides that form on the magnesium surface, and we assume that iron and chloride ion overcome such passivity. The Mg surface layer has been shown to comprise both MgO and $Mg(OH)_2$ and to have small bits of elemental magnesium embedded within.[9] We surmise that the role of iron is to facilitate magnesium oxidation by serving as a conduit for electrons, or by producing reactive iron species that shuttle between valence states and in effect transfer electrons to the solution, or by promoting the dissolution of the surface oxide/hydroxide structure. However, magnesium so activated cannot react unless it is brought into contact with water. We further surmise that the role of NaCl in catalyzing the reaction is to generate channels through the $Mg(OH)_2$ layer, presumably by replacing hydroxide ion with chloride ion to form the more soluble Mg(OH)Cl and to weaken the lattice, thereby allowing water to penetrate through to the unreacted magnesium surface. Once the magnesium−water reaction starts, it becomes self-sustaining. Its rate would be controlled by the number of surface sites with access channels to water, consistent with first-order saturation kinetics (Figure 1).[10,11]

Elementary Steps in the H_2 Formation Mechanism. The stoichiometry of reaction 1 gives no hint of the complex set of elementary reactions that ultimately leads to the formation of dihydrogen. These reaction steps involve physical and chemical processes that occur heterogeneously and very rapidly. First and foremost is transfer of electrons from the metal surface to the aqueous medium, which results in the formation of trapped electrons, both fully solvated, e_s^- , or only partially solvated electrons, e_p^-, which then in subpicoseconds become fully solvated electrons. These transient entities will tend to be located close to the solid surface, but some will diffuse into the bulk of the solution leading to a nonhomogeneous distribution about the metal surface. These formation and diffusion processes and the subsequent bimolecular reactions of the formed and diffusing transient entities, which have been studied extensively in radiation chemistry, are summarized as follows:

$$Mg(s) \rightarrow 2e_p^- (e_s^-) + Mg^{2+} \quad (2)$$

$$e_p^- \rightarrow e_s^- \quad (3)$$

$$e_s^- + H^+ \rightarrow H^\bullet \quad (4)$$

$$e_s^- + e_s^- \rightarrow H_2 + 2OH^- \quad (5)$$

$$e_s^- + H^\bullet \rightarrow H_2 + OH^- \quad (6)$$

$$H^\bullet + H^\bullet \rightarrow H_2 \quad (7)$$

This scheme indicates that the reduction of water by magnesium need not involve the direct formation of H_2 on the surface of the metal but can proceed through reactions in the solution near the surface. Moreover, it implies that the potential exists for suppressing H_2 formation if solutes with high enough reactivity toward e_p^- , e_s^-, or $H^\bullet$ can scavenge these transient entities to form other reactive intermediates that eventually yield stable products other than H_2.

Scavenger Studies. *Scavenger Dependence.* A comparison of H_2 yields for different scavengers at comparable concentrations shows that the higher the reactivity toward either e_s^- or $H^\bullet$ (Table 1), the lower the H_2 yield (Figure 2). Without any scavenger present, as indicated by the control, the cumulative volume of H_2 at reaction's end normalized to 0.100 g Mg(Fe) is 89.8 mL. Addition of monochloroacetate ion, a relatively good electron scavenger that reacts by dissociative electron attachment, decreases the yield. With trichloroacetate ion (TCA), an even better electron scavenger because of the totally chlorinated C-2, the yield decreases further. Electrons react more rapidly with persulfate ion and the yield is even lower. Though not shown in Figure 2, other electron scavengers also lower the H_2 yield relative to the control. For example, addition reactions of solvated electrons at the carbonyl group of pyruvate ion ($k(e_s^-)$ $= 6.8 \times 10^9$ M^{-1} s^{-1}), at the double bond of maleate ion ($k(e_s^-) = 2.9 \times 10^{10}$ M^{-1} s^{-1}), and at the benzene ring of benzoate ion ($k(e_s^-) = 3.3 \times 10^9$ M^{-1} s^{-1}), all lead to suppressed H_2 yields.[12] These solutes are also reactive to $H^\bullet$ at the same sites of attack. Scavenging both of these precursors of dihydrogen should enhance suppression, as inspection of Figure 2 and Table 1 shows.

TABLE 1: Rate Constants for Scavenger Reactions with Aquated Electrons and H-Atoms[a]

reaction	$k(H^\bullet$ or $e^-_s)$ (M^{-1} s^{-1})
$e^-_s + CH_2ClCOO^- \rightarrow Cl^- + {}^\bullet CH_2COO^-$	1.0×10^9
$e^-_s + CCl_3COO^- \rightarrow Cl^- + {}^\bullet CCl2COO^-$	8.5×10^9
$e^-_s + S_2O_8^{2-} \rightarrow SO_4^{2-} + SO_4^{\bullet -}$	1.2×10^{10}
$e^-_s + NO_3^- \rightarrow NO_3^{\bullet 2-} \xrightarrow{H^+} NO_2 + OH^-$	9.7×10^9
$H^\bullet + NO_3^- \rightarrow HNO_3^{\bullet -} \rightarrow NO_2 + OH^-$	1.0×10^7
$e^-_s + NO_2^- \rightarrow NO_2^{\bullet 2-} \xrightarrow{H^+} NO + OH^-$	3.5×10^9
$H^\bullet + NO_2^- \rightarrow HNO_2^{\bullet -} \rightarrow NO + OH^-$	7.1×10^8
$e^-_s + Cu^{2+} \rightarrow Cu^+$	3.8×10^{10}
$H^\bullet + Cu^{2+} \rightarrow Cu^+ + H^+$	9.1×10^7

[a] All entries from Ross, A. B.; Mallard, W. G.; Helman, W. P.; Buxton, G. V.; Huie, R. E.; Neta, P. *NDRL-NIST Solution Kinetics Database:-Ver. 3.0*; Notre Dame Radiation Laboratory, Notre Dame, IN, and National Institute of Standards and Technology, Gaithersburg, MD (1998).

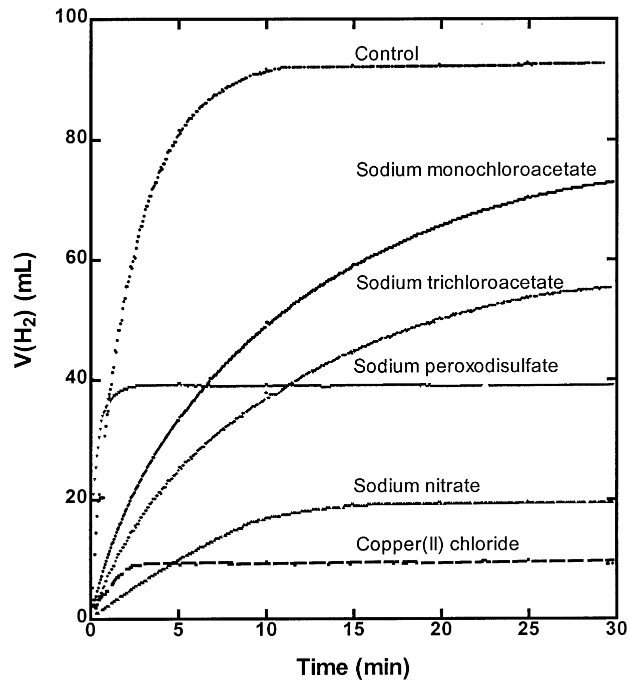

Figure 2. H_2 evolution vs time with different scavengers, all at approximately 1 M concentration. The volume is normalized to 0.100 g Mg(Fe). (The plots are based on smooth curves drawn through experimental data, which were then digitized. Symbols do not represent data points.)

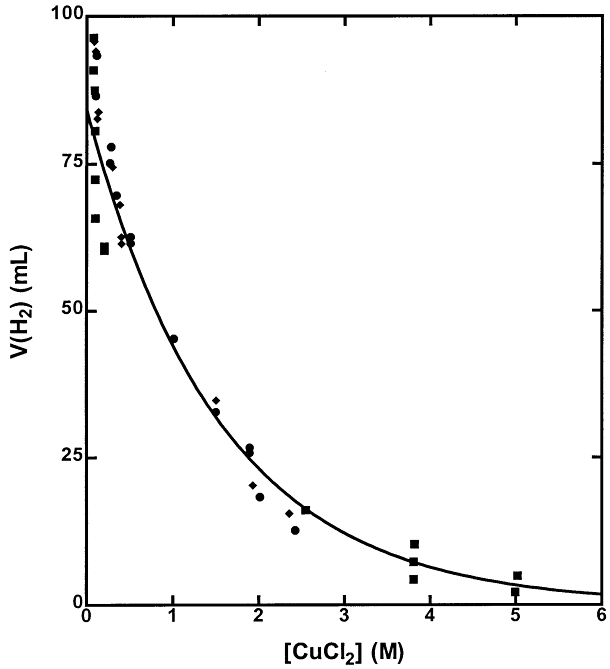

Figure 3. Decrease in H_2-yield (normalized to 0.100 g Mg(Fe)) with increasing [$CuCl_2$]. Experimental data: (■) pH 1.0, (●) pH 1.8, (◆) pH 2.0. Calculated curve (Hunt relation modified for this experiment): Volume of H_2 = 84.18 exp(−[$CuCl_2$]/1.55).

Adding nitrate ion, a good electron scavenger but only a moderately effective $H^•$ scavenger, further depresses the H_2 yield relative to persulfate ion. Nitrite ion (not shown) is likewise effective. Upon being reduced to metallic copper(0), copper(II) ion, which scavenges both $H^•$ and e_s^- efficiently, suppresses H_2 to 8 mL. For copper(II) ion in high acid ($[H^+] \geq 1$ M) where e_s^- is scavenged by H^+, the H_2 is suppressed, but less effectively, because copper(II) ion is reacting with $H^•$, with which it has a lower rate constant than it does with e_s^- and consequently requires a higher concentration to be effective.

Scavenger Concentration Dependence. Although the H_2 yield and time to completion of reaction clearly decrease with increasing scavenger concentration, the decrease is not linearly proportional to the increase in scavenger concentration. For nitrate and several other scavengers suppression of about 90% of the control volume of H_2 gas at very high concentrations on the order of 2−5 M implies that almost all the precursors are scavengeable and that they are not uniformly distributed in solution, but exist for a short time in the water near the interface between the iron-activated magnesium particle and the solution.

The dependence of H_2-yield on scavenger concentration can be explained by a comparison with the effect of scavengers on the yield of products from the radiolysis of aqueous solutions. A semilogarithmic relationship has been demonstrated between the decrease in the observed yield of nonhomogeneously distributed solvated electrons and scavenger concentration.[13,14] Similar excellent semilogarithmic correlations are obtained here between the decrease in the observed H_2-yield and scavenger concentration. The relative effectiveness of each scavenger studied can be estimated from plots such as Figure 3, by defining the concentration at which only 37% of precursors remains unscavenged, namely, C_{37}. For solutions of pH ≥ 2, C_{37}(Cu(II)) is 0.2 M (Figure 3), whereas for pH ≤ 2 it is about 7-fold higher.

Multiple Scavenger Solutions: Evidence for $H^•$. Because the initiating event in the reduction of water by magnesium is the release of an electron, it is possible that no H-atoms are formed. To determine if, and to what extent, H-atoms are formed and correspond to precursors of H_2, competitive scavenging experiments were performed.[15] These experiments were designed to favor involvement of $H^•$ by removing a large fraction of the e_s^- formed, thus minimizing its involvement as an H_2 precursor. Removal of e_s^- is effected in one of two ways. For $H^•$ scavengers such as Cu(II) that also react with e_s^- at (or close to) the diffusion-controlled rate, the $H^•$ scavenger also removes e_s^-. For $H^•$ scavengers that react with e_s^- at less than the diffusion-controlled rate, 1 M TCA is added to the reaction mixture. Two different but competitive $H^•$ scavengers are present in each reaction system. One scavenger reacts with $H^•$ to form H_2; the other also reacts with $H^•$, but not to form H_2. For a fixed concentration of the H_2-forming $H^•$ scavenger, increasing the concentration of the scavenger that forms no H_2 should decrease the H_2 yield. The concentration of H_2-forming competitive scavenger ethanol reacting according to reaction 8

$$H^• + CH_3CH_2OH \rightarrow CH_3C^•HOH + H_2 \qquad (8)$$

is kept fixed at a constant value, usually 2 M. The concentration of non-H_2-forming competitive scavenger, represented by X and reacting according to reaction 9

$$H^• + X \rightarrow HX^• \qquad (9)$$

is varied.

If $H^•$ is formed, it is reasonable to expect that some geminate recombination of $H^•$ occurs regardless of how high the total scavenger concentration may be. As a result, a portion of the measured volume of H_2 formed may not be susceptible to scavenging. This portion is therefore irreducible. The pathway yielding a *constant*, irreducible, scavenger-unaffected H_2 is referred to as *irreducible*, the pathway yielding a *variable*, scavenger-affected H_2 is referred to as *reducible*, and rate constants for these two pathways are designated *k*(irreducible) and *k*(reducible), respectively. It is possible to determine whether H-atoms are formed and to partition the H_2 yield into *irreducible* and *reducible* pathways as shown below.

For a fixed [C_2H_5OH] and for homogeneously distributed reactants, decreasing the ratio [C_2H_5OH]/[X] should decrease the cumulative H_2 volume as follows. Let V_T be the total volume of H_2 gas at the end of the reaction, V_E the volume of H_2 gas formed at the specified amount of ethanol present, and V_F the irreducible volume of H_2 gas associated with reaction 8. Per mole of Mg(Fe) initially present, the added competitive $H^•$ scavenger effectively reduces V_E and decreases V_T according to eq I:

$$V_T = V_F + fV_E \qquad (I)$$

where $f = k_E\,[C_2H_5OH]/(k_E\,[C_2H_5OH] + k_X[X])$, k_E the rate constant for scavenging by ethanol, and k_X the rate constant for the non-H_2-forming competitive scavenger, X. Applying the steady-state assumption to $H^•$ in reactions 8 and 9 gives, per mole Mg(Fe) initially present, eq II:

$$\frac{1}{V_T - V_F} = \frac{1}{V_E} + \frac{R}{V_E}\frac{[X]}{[C_2H_5OH]} \qquad (II)$$

where $R = k_X/k_E$. This equation is comparable to those used in radiation chemistry to study the competition for transient species homogeneously distributed in the bulk solution. Accordingly, a plot of $1/(V_T - V_F)$ against [X] should be linear at constant

$[C_2H_5OH] = 2$ M. No such linear relation was found for any competitive scavenger that was studied.

This deviation from linearity associated with the magnesium−water reaction is in part a consequence of complicating side effects. Addition of $H^\bullet$ to double bonds or aromatic rings of organic scavengers can lead to products that subsequently eliminate H_2 as a byproduct on a time scale comparable to that of the magnesium−water reaction. In these cases a reliable measure of V_T is not possible. For such scavengers, however, it is possible to find a concentration range where the H_2-yield is reduced compared with control, but byproduct H_2 formation is insignificant. Even an inorganic scavenger such as hexacyanoiron(II) anion did not behave as expected. In this case, the reaction appeared to be slower than anticipated; plateaus in gas volume expected at 30 min, were not reached in 120 min. After screening several potential candidates, copper(II) sulfate and sodium benzoate ($NaC_6H_5CO_2$) were selected as competitive scavengers. Competitive scavenging experiments with the latter were kept below 0.1 M, since slow evolution of H_2 gas was observed at higher concentrations. For these two scavengers, increased [X] decreased V_T, but even with precautions regarding scavenger concentration and pH, the plots according to eq 2 were curved. Moreover, the value of R obtained was quite different from the expected value based on literature values.[12] The nonlinearity and poor agreement for R presumably reflect a more fundamental influence of nonhomogeneously distributed reactants.

There is considerable evidence from scavenger studies in radiation chemistry processes that at high concentrations these scavengers react with nonhomogeneously distributed e_s^- and precursors of e_s^- to influence final radiolysis product yields.[16] Applying this concept to reactions occurring near the magnesium-solution interface explains why eq II is inadequate. If the nature and lifetime of precursor entities formed upon transfer of electrons into the solution are affected by the presence of scavengers, then the effective yields of e_s^- and $H^\bullet$ will differ depending on the type and concentration of scavenger. Therefore, the assumption that V_E is reduced simply by $(1 - f)$ will be untenable. These considerations suggest that the competitive scavenging data could be analyzed by modeling the reactions using a variable e_s^- and $H^\bullet$ formation stoichiometry. Mechanisms have been devised using elementary reaction steps with known rate constants and fitted values for the following magnesium−water reduction reaction 10:

$$Mg + 2H_2O \rightarrow Mg(OH)_2 + e\,e_s^- + hH^\bullet \qquad (10)$$

The sum of the stoichiometric coefficients e and h in reaction 10 is taken as ≤2. A successful mechanism must fit *both* the kinetics of H_2 formation and the final H_2 yield.

For competitive benzoate vs ethanol scavenging of $H^\bullet$, the modeling initially considered a twelve-step mechanism and assumed values of $e = 0.7$ and $h = 1.3$. In addition to reaction 10, a group of 10 reactions was considered: e_s^- reacting with e_s^-, H^+, $H^\bullet$, H_2O, $C_6H_5CO_2^-$, TCA, and C_2H_5OH; and $H^\bullet$ reacting with $H^\bullet$, $C_6H_5CO_2^-$, and C_2H_5OH. The scavenger-unaffected *irreducible* formation of H_2 was accounted for by reaction 1. This mechanistic model was compared against actual data and values for k(reducible), e, and h (corresponding to reaction 10) and k(irreducible) (corresponding to reaction 1) were obtained by nonlinear curve-fitting.[17] In the presence of ethanol and benzoate anion, k(reducible) ≥ 1000k(irreducible). Formation of H_2 by direct (geminate or some other surface-influenced) reaction is negligible. In an effort to further simplify

TABLE 2: Competitive Scavenging Models:

reaction	rate constant
(A) Benzoate ($C_6H_5CO_2^-$) vs Ethanol (C_2H_5OH) with Trichloroacetate ($Cl_3CCO_2^-$)[a]	
$Mg + 2H_2O \rightarrow Mg(OH)_2 + 1.24H^\bullet + 0.25\ e^-_s$	2.18×10^{-3} (s^{-1})
$e^-_s + Cl_3CCOO^- \rightarrow Cl_2C^\bullet COO + Cl^-$	8.5×10^{9} ($M^{-1}\ s^{-1}$)
$H^\bullet + C_6H_5COO^- \rightarrow {}^\bullet C_6H_6COO^-$	9.2×10^{8} ($M^{-1}\ s^{-1}$)
$H^\bullet + C_2H_5OH \rightarrow CH_3C^\bullet HOH + H_2$	1.7×10^{7} ($M^{-1}\ s^{-1}$)
(B) Copper(II) Sulfate ($CuSO_4$) vs Ethanol	
$Mg + 2H_2O \rightarrow Mg(OH)_2 + 1.95H^\bullet$	7.19×10^{-3} (s^{-1})
$H^\bullet + Cu^{2+} \rightarrow Cu^+$	9.1×10^{7} ($M^{-1}\ s^{-1}$)
$H^\bullet + C_2H_5OH \rightarrow CH_3C^\bullet HOH + H_2$	1.7×10^{7} ($M^{-1}\ s^{-1}$)

[a] Experimental conditions as in Figure 5; last rate constant multiplied by 6.12×10^2 (A), and 1.22×10^3 (B) to convert molar concentration to volume (mL) in H_2 formation step; stoichiometric coefficients and rate constant for magnesium reaction are fitted values.

the mechanism, the rate of each reaction was calculated over the time frame of the experiment and the logarithm of the rate plotted against time. The fastest among the 10 reactions is e_s^- + TCA. Compared with the rate of this reaction, the remaining reactions could be sorted into three subgroups. The slowest reacting subgroup comprised the radical−radical reactions $e_s^- + e_s^-$, $e_s^- + H^\bullet$, and $H^\bullet + H^\bullet$, which were no more than 10^{-10} as fast as e_s^- + TCA. A second subgroup comprised reactions $e_s^- + C_2H_5OH$, $e_s^- + H_2O$, and $e_s^- + H^+$ that were of comparable rates, about 10^{-7} as fast as e_s^- + TCA. Both subgroups of reactions were considered to be too slow to influence measurements of accumulated H_2 yield and accordingly were dropped from consideration (as was the *irreducible* H_2 pathway, for reasons given above).

The resulting four-step mechanism was fitted to the data. Values for k(reducible), e, and h were allowed to vary in the curve-fitting procedure (Table 2A, Figure 4A). In two experiments with sodium benzoate concentrations of 0.063 and 0.125 M, h increased from 1.24 to 1.56 and e decreased from 0.25 to 0.10. Reaction of e_s^- with $C_6H_5CO_2^-$ does not appear in Table 2, because this reaction cannot compete with TCA for e_s^-. It would compete favorably at higher $[C_6H_5CO_2^-]$, but then the byproduct elimination of H_2 would seriously complicate measurement of dihydrogen formed initially from the $Mg-H_2O$ reaction. The H_2 elimination reaction was not included in the model.

An eleven-step mechanism was used to model competitive copper(II) vs ethanol H-atom scavenging. In addition to reactions 1 and 10, nine reactions were considered: e_s^- reacting with e_s^-, H^+, $H^\bullet$, H_2O, Cu^{2+}, and C_2H_5OH; and $H^\bullet$ reacting with $H^\bullet$, Cu^{2+}, and C_2H_5OH. As in the benzoate ion case, the modeling initially considered the full mechanism, included assumed values of $e = 0.7$ and $h = 1.3$, and computed the rate of each reaction over the time frame of the experiment. The rate of reaction 1 was insignificant; the rate of reaction 10 was fastest; the rates of the three radical−radical reactions $e_s^- + e_s^-$, $e_s^- + H^\bullet$, and $H^\bullet + H^\bullet$ were considerably slower, being 10^{-9} to 10^{-14} times the rate of reaction 10. The rates of reactions of e_s^- with C_2H_5OH and H_2O were also slower, being approximately 10^{-7} times the rate of reaction 10. These five reactions were dropped from consideration.

A simpler five-step mechanism was fitted to the data, by varying k(reducible), e, and h. Compared with sodium benzoate, copper(II) sulfate speeds up the overall reaction (Figure 4B), corresponding to higher rate constants for k(reducible) (Table 2B) at comparable initial amounts of Mg(Fe). In one series of investigations, seven experiments with copper(II) sulfate con-

TABLE 3: Fitting Results for H_2-Production from Reducible and Irreducible Models[a]

scavenger	[scavenger][b] (M)	k(reducible) × 1000 (s^{-1})	k(irreducible) × 1000 (s^{-1})	final irreducible V (mL)[c]	final total V (mL)
none	0.0	5.29	0.2	0.8	89.8
sodium benzoate, ethanol, sodium trichloroacetate	$[C_6H_5CO_2^-]$ =0.063, $[C_2H_5OH]$ = 2.00, $[Cl_3CCO_2^-]$ = 1.00	2.13	2.16×10^{-2}	0.02	24.4
copper(II) sulfate, ethanol	[Cu(II)] = 0.006, $[C_2H_5OH]$ = 6.00	2.67	8.2×10^{-5}	0.1	95.0
copper(II) chloride	[Cu(II)] = 0.04	3.5	5.0	5.5	64.6
copper(II) chloride	[Cu(II)] = 0.12	5.78	5.4	33.8	43.9
copper(II) chloride	[Cu(II)] = 0.5	20	2.3	9.6	9.6
sodium nitrate	$[NO_3^-]$ = 0.01	0.44	3.9	60.7	85.6
sodium nitrate	$[NO_3^-]$ = 0.1	1.9	3.4	50	50

[a] All reactions scaled to 0.1 g Mg(Fe) in 2.0 M NaCl solution. [b] Initial concentrations. [c] Measured at a time chosen so that the rates of both models are measurable and competitive; e.g., 250 s for $[CuCl_2]_0 = 0.12$ M.

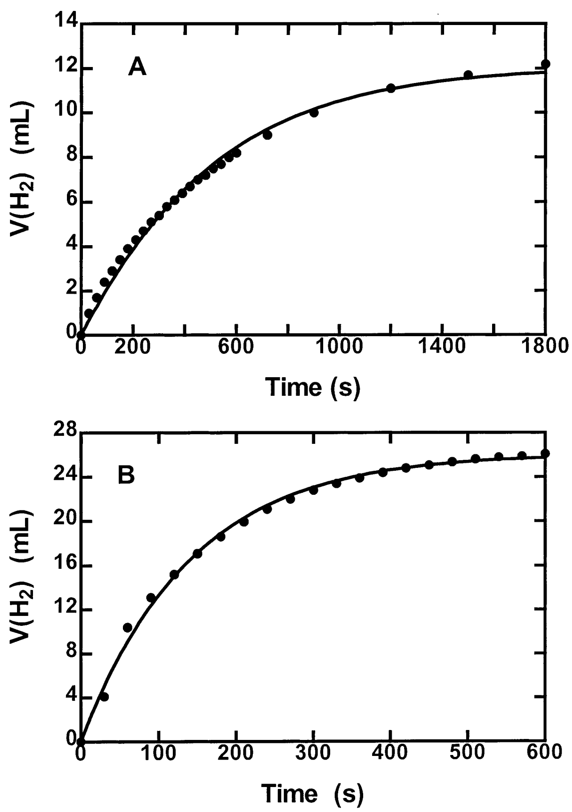

Figure 4. Competitive scavenging model: experimental data (●), curve (−) computed from model in Table 2. Experimental conditions: (A) 0.0502 g Mg(Fe) powder, 0.063 M $NaC_6H_5CO_2$, 2 M ethanol, 1 M TCA, solution volume 25 mL, room temperature 26.3−27.8 °C, barometric pressure 1.01×10^5 Pa, initial pH 7.30, final pH 11.46; (B) 0.025 g Mg(Fe) powder, 2 M NaCl, 0.25 M $CuSO_4$, 2 M ethanol, solution volume 50 mL, room temperature 29.8−30.2 °C, barometric pressure 9.95×10^4 Pa, pH 2.5.

centrations from 0.006 to 0.25 M were carried out. The value of *e* decreases with increasing $[Cu^{2+}]$; above 0.06 M $CuSO_4$ the value of *e* is essentially equal to zero. With so little e_s^- available, none of the remaining e_s^- reactions contributes appreciably to the overall reaction. Accordingly, these steps were omitted, and the resulting three-step model that was used fitted the data very well (Table 2B, Figure 4B).

For competitive scavenging, a clear trend is implied regarding the significant involvement of e_s^- and $H^\bullet$ and the insignificant involvement of the *irreducible* pathway. Both of the $H^\bullet$ scavengers used in these studies, benzoate and copper(II) ions, are also excellent e_s^- scavengers, with copper(II) ion being over 10 times more effective than benzoate ion. Consistent with these reactivities, the yield of e_s^- decreases with increasing scavenger concentration and the yield of H_2 falls essentially to zero at $[Cu^{2+}] \geq 0.06$ M. The final yield of H_2 and the kinetics of its formation in ethanolic solutions containing efficient e_s^- scavengers are controlled presumably by the rate of electron transfer from magnesium or iron metal into the water as well as by the relative rates of $H^\bullet$ scavenging by ethanol and by benzoate or copper(II) ions. On the basis of these competitive scavenger studies, we conclude that e_s^- and $H^\bullet$ are both significant precursors of H_2 in the elementary step mechanism of the Mg−H_2O reaction.

Single Scavenger Solutions: Evidence for e_p^- and e_s^-. Results for single scavengers acting alone, e.g., copper(II) (Table 3), can be explained by the simplified mechanism with inclusion of the *irreducible* pathway. For example, for 2.66×10^{-3} mol Mg(Fe) in 2.0 M sodium chloride solution with 0.5 M copper(II) sulfate and initial pH 2.59, the final volume of H_2 is 9.6 mL, compared with 23 mL final volume for the same reaction with no copper(II) sulfate present. The kinetics curves for such reactions are successfully modeled with a five-step mechanism: reactions 1 and 10, e_s^- scavenged by Cu^{2+} and H^+, $H^\bullet$ scavenged by Cu^{2+}.

The potent effect of nitrate ion concentration on reducing the formation of dihydrogen is characterized by a $V(H_2)$ vs $[NaNO_3]$ plot that is the sum of two exponentials. Nitrate ion is not only a good e_s^- scavenger, but also the reaction product is nitrite ion, which scavenges both e_s^- and $H^\bullet$. To avoid complicating the results by either depleting the nitrate ion or introducing secondary scavenging by nitrite ion, special precautions were taken to maintain nitrate ion in excess over Mg(Fe). Very high nitrate ion concentrations had to be avoided, however, because nitrate ion, like other oxidizing anions such as chromate and phosphate, forms a protective film on the magnesium surface which decreases the rate of magnesium ion formation.[18] Accordingly, the volume of solution and/or the weight of Mg(Fe) used were judiciously chosen so that the molar ratio of nitrate ion to Mg was always greater than 2.5 and ran as high as 25. The resulting plot is shown in Figure 5. A very sharp reduction in dihydrogen is followed by a more gradual reduction. On the basis of a fitting to the sum of two exponentials, C_{37} values for the sharp and gradual reductions in the yield of dihydrogen of 0.1 and 1.8 M, respectively, were obtained. A reasonable fit to the sum of two exponentials with a residual dihydrogen yield was also obtained, suggesting that an *irreducible* pathway might also be involved.

These results are consistent with the mechanistic model, provided that an additional reaction is added to account for scavenging of e_p^- as in reaction 11, where X is any scavenger,

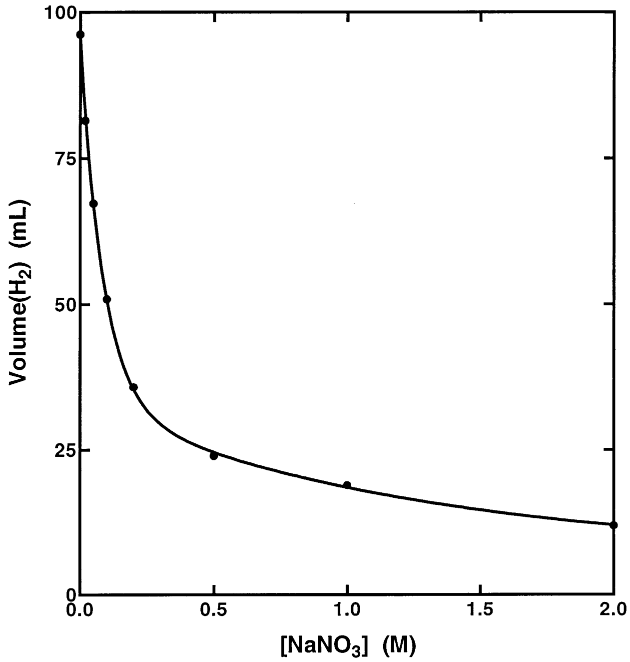

Figure 5. Decrease in H_2 yield (normalized to 0.100 g Mg(Fe)) with increasing [$NaNO_3$]; calculated curve is the sum of two exponentials (see text).

and *n* is zero

$$e_p^- + X^n \rightarrow X^{n-1} \qquad (11)$$

or any positive or negative charge. The very sharp reduction at low [$NaNO_3$] reflects the efficient scavenging of e_s^- by NO_3^- and the rapid conversion of e_p^- to e_s^-. At higher [$NaNO_3$], reaction 11 begins to compete with reaction 3, but any e_s^- formed is rapidly scavenged by nitrate ion. Consequently, the dihydrogen yield is substantially reduced, but further reduction is expected to be gradual because much higher [$NaNO_3$] would be needed to compete effectively against reaction 3. (As mentioned above, very high nitrate ion concentration passivates Mg and could not be used.)

For scavenging with a single solute, the relative involvement of the *reduced* and *irreducible* pathways is less obvious to discern. When copper(II) acts as a single scavenger, the *irreducible* pathway is significant, and when sufficient copper(II) is present to scavenge virtually all precursors ([Cu(II)] = 0.5 M), this pathway accounts for all the H_2 produced (Table 3). Compared with the competitive and copper(II) studies, the nitrate results are significantly different. For nitrate ion *k*(irreducible) ≫ *k*(reducible*)* (Table 3) and the direct pathway is enhanced. As noted above, nitrate ion, or its reaction products such as nitrite ion, influence magnesium surface properties.

Thermochemistry. Besides suppressing H_2 formation from the reaction of magnesium with water, the interactions of scavengers with H-atoms and solvated electrons also affect the thermochemistry of the overall reaction. For comparative purposes, the overall reaction was monitored calorimetrically for three representative scavengers. The fraction of precursors scavenged was the same in each case, because a similar C_{37} concentration was used for each scavenger. Compared with the scavenger-free control, the presence of scavenger generated more heat (Figure 6). These results are consistent with the model (Table 2), which implies a change in stoichiometry: in the presence of scavengers, water is no longer exclusively reduced. A more detailed consideration of the thermochemistry when copper(II) is used illustrates the effects.

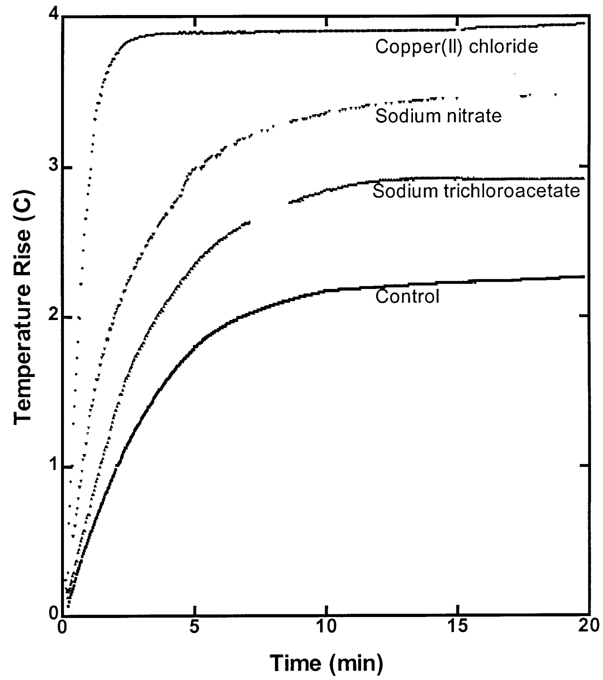

Figure 6. Temperature rise due to heat generation in the magnesium–water reaction with different scavengers present. Initial concentrations: sodium nitrate 0.2 M, sodium trichloroacetate 0.5 M, copper(II) chloride 1.5 M. The temperature rise is normalized to 0.100 g Mg(Fe). (The plots are based on smooth curves drawn through experimental data, which were then digitized. Symbols do not represent data points.)

Reduction of Cu^{2+} ion by e_s^- or $H^•$ leads to Cu^+ ion, elemental copper (Cu^0), or a mixture of both, depending on the amount of magnesium, the pH, and [copper(II)]. In experiments involving acidic solutions and an excess of Cu^{2+} ion over Mg, the heat generation is enhanced more than 70% over the control reaction of magnesium with water in the absence of scavenger. This observation is consistent with formation of Cu^0 according to the following overall stoichiometry:

$$Mg + CuCl_2 \rightarrow Mg^{2+} + Cu + 2Cl^- \qquad (12)$$

The calculated heat of reaction 12 is 582.29 kJ mol^{-1} at 25 °C, which is almost twice that of the copper-free, control reaction.

Comparison with Radiolytic and Other Data. Identifying e_s^- as a precursor of H_2 allows one to compare the effectiveness with which scavengers function in two quite different phenomena—the reduction of water by magnesium and the radiolysis of water—and in turn to show that both phenomena have in common the same short-lived intermediates and many of the same elementary steps. This commonality could involve e_p^-, the presumed precursor of e_s^- (reaction 3). Comparing the effectiveness of scavengers of e_p^- and/or e_s^-, is illustrative.

Using picosecond pulse radiolysis, Hunt and co-workers monitored the optical absorption and therefore the primary yield of e_s^- immediately following such short stroboscopic pulses.[13] The presence of scavengers decreased both the yield and lifetime of e_s^-.[13] From these results Hunt and co-workers obtained C_{37} values for scavenging e_p^- and $k(e_s^-)$ values for the reactions of scavengers with e_s^- at high scavenger concentrations. A plot of C_{37} vs $k(e_s^-)$ showed a good correlation. Using the completely different technique of positron annihilation lifetime spectroscopy, in which positronium is formed in extremely short times,[19] Duplâtre and Jonah studied the effect of scavengers on the reaction between positrons and electrons. From the inhibition

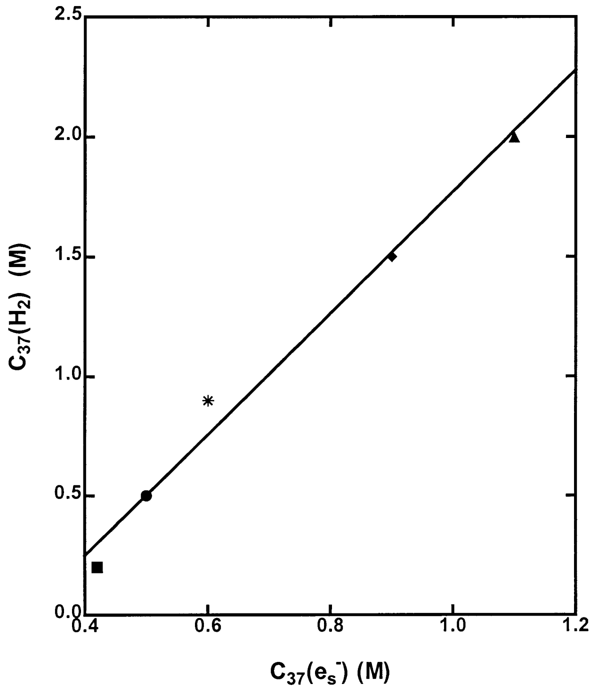

Figure 7. Comparison of C_{37} for H_2 yield from the reduction of water by iron-activated magnesium (this study) with C_{37} for e_s^- formation in pulse radiolysis: ■, nitrate (ref 14); ●, TCA (ref 13); *, peroxodisulfate (ref 17); ◆, copper(II) (ref 14); ▲, maleate (ref 17). A linear least-squares line connects the data points.

of positronium formation by scavengers, they showed that the inhibition rate constants correlated both with the reciprocals of their C_{37} values and with the corresponding values for e_s^- formation from pulse radiolysis experiments. These correlations led them to conclude that e_p^- was being scavenged in the positronium experiments as well as in the radiolytic experiments. A similar relationship has been found in pulse irradiated alkaline glasses (I. A. Taub, unpublished data), but for times much longer than those measured in solution.[20]

If the precursors reacting with scavengers in the thermal reaction of magnesium with water are similar to precursors reacting with scavengers in the radiation chemistry studies, the C_{37} values from the two separate groups of studies should correlate. Accordingly, C_{37} values for H_2 formation have been plotted against C_{37} values for e_s^- formation (Figure 7). Though the set of scavengers common to all three techniques (pulse radiolysis, positron annihilation, magnesium−water) is small, the plot shows a relatively good correlation, consistent with scavenging e_p^-, although it could reflect some scavenging of e_s^- as well. This mechanistic model posits mobile, solution-bound electrons as the initiators of chemical events leading to the formation of H_2, as was also suggested in some earlier investigations into the mechanisms of electrochemical and chemical reduction by powerful reductants such as sodium amalgam.

In one study by Hughes and Roche,[21] electron scavengers reduced the H_2 yield produced upon adding sodium amalgam to water. The reduction in H_2 yield was attributed to competition between scavenger and H^+ for e_s^-. In another study by Walker,[22] in which H_2 and N_2 were measured in the presence of N_2O (which dissociatively attaches e_s^- to produce N_2), similar results were obtained when generating the presumptive e_s^- by adding sodium amalgam, by using electrode processes, and by reducing water with U^{3+} upon adding solid UCl_3 to the solution. In a spectroscopic study of water electrolysis, e_s^- was detected in solution, very close to a polished silver electrode.[23] Moreover, the involvement of e_s^- and its addition to the benzene ring were inferred in studies of electrolytic reductions in ethanolic solutions containing hexamethylphosphoramide.[24] Clearly, these conventional chemical and electrochemical reduction processes generate a common e_s^-, but in different ways and with different distributions and lifetimes.

The similarity in the formation of solvated electrons as water reacts with Mg and as water is photolyzed or radiolyzed is remarkable. It implies that, despite the enormous differences in the energies involved and in the mode of energy deposition, some common entities and processes are involved. The existence of favorable configurations of water molecules that can trap so-called quasi-free electrons, e_{qf}^-, appears to be the key factor. In the radiolysis of water, high energy photons and electrons penetrate through the water and ionize some molecules, creating positive ions and ejected electrons, which eventually equilibrate thermally and become quasi-free. Although the details are still being worked out,[25] quasi-free electrons[26−29] are simultaneously weakly bound in shallow traps and strongly bound in deeper traps that become further stabilized, corresponding to e_s^-. The distance involved must be very short. The conclusion is that traps accommodate electrons irrespective of their source.

The similarity in the effect of added solutes on the yield of dihydrogen in the radiolysis of water and in the magnesium−water reaction is even more remarkable. Both processes seem to involve solutes scavenging the solvated electron and its precursor(s). In recent radiolytic studies, Pimblott and co-workers[30,31] have shown that, despite the long-standing assumption of a fixed and irreducible yield of geminate dihydrogen, many solutes at high concentrations can significantly reduce this yield. In the magnesium−water reaction, many solutes are clearly capable of scavenging e_s^- as well as its precursor.

Generalized Concepts. Based on the foregoing, one can generalize the concepts underlying both the reaction of iron-activated magnesium with water in chloride-containing solutions to form dihydrogen and the effectiveness with which certain solutes suppress hydrogen formation. These concepts relate to the transfer of electrons into the solution, the consequent modification of the magnesium surface, the time-dependent redistribution of reactive entities near the magnesium-solution interface, and the reaction of solutes with homogeneously distributed reactive entities in the bulk solution.

The electron transfer process must occur near where iron contacts the magnesium surface and presumably involves a short range interaction with a favorably configured collection of water molecules. Comparable processes in radiolysis and photolysis generate precursors of the solvated electron, such as the p-state electron or the less specific e_{pre}^-. It is reasonable to assume that the distribution of distances of these electrons from the magnesium surface is exponential, the range of which is less than that observed for the photoejection of electrons from other metallic surfaces.[32]

After electron transfer, the magnesium surface becomes modified, as a consequence of lattice alteration, product formation, and pH increase. Transfer of an electron from a magnesium atom creates a lattice defect that weakens the metal's structure and favors subsequent electron transfer at or near the surface. In control solutions containing just chloride, the products are Mg^{2+} and OH^-, which raises the pH to about 11. The chloride ion readily replaces hydroxide ion; it reacts with $Mg(OH)_2$, for example, forming the more soluble MgOHCl or $MgCl_2$, thereby causing channels in the precipitate and in the oxide/hydroxide layer through which water can reach the magnesium. In keeping with the observed kinetics, this channeling effect becomes more extensive as chloride concentration increases, but the effect of chloride levels off when the surface becomes sufficiently porous that the rate-determining process is availability of reactive magnesium lattice sites. If an acidic solution is used, such as HCl or even $CuCl_2$, which hydrolyzes extensively lowering the pH to 2, the precipitate does not form and the oxide/hydroxide layer is rapidly removed, so the magnesium surface is readily available for further reaction. Accordingly, reaction 10 is faster when copper(II) solutions are used. Moreover, the phenomenological rate of dihydrogen formation will depend on the total availability of unreacted magnesium sites, which will generally increase with increasing surface area. Consequently, the reaction rate normalized for the same mass of magnesium is slowest when the Mg(Fe) is shaped as a plate or cylinder and fastest when left as small particles (I. A. Taub et al., unpublished data).

The nonhomogeneous distribution of the transient precursor and resultant electron entities in the vicinity of the interface between magnesium and solution will change with time, because reactions involving these entities occur on a time scale comparable to diffusion away from the sites of their formation. Thermodynamic values obtained from measurements on equilibrated homogeneous systems should be applied cautiously, if at all, to individual steps in such mechanisms. Nevertheless, it is worthwhile considering the free energy change of reaction 2, the mechanism's rate-determining step. Using available thermodynamic data leads to an unfavorable free energy change for this reaction. The reverse of reaction 2 involves a sequence of two elementary steps. If we assume the reverse steps are rapid, possibly diffusion controlled, and apply the steady-state concept to $[Mg^+]$, we can calculate the rate constant of the forward step from the mass action law. This rate constant should be equal to the observed rate constant, *k*, defined above. With $K_2 = 3.15 \times 10^{-18}$ M^2, and the third-order reverse rate constant approximately equal to 1×10^{15} M^{-2} s^{-1}, we calculate a forward rate constant approximately 3×10^{-3} s^{-1}, consistent with *k* (Figure 3).

The e_s^- and $H^\bullet$ that survive reaction near the magnesium–solution interface and become homogeneously distributed throughout the solution then undergo competitive kinetic reactions that further influence the nature and amount of final products, including H_2. The relative amounts of e_s^- and $H^\bullet$ that appear in the bulk solution, however, will be significantly affected by the reactivity and concentration of scavengers. These concepts were considered in developing a chemical heater based on the Mg(Fe) reaction with water in which 70% more heat is generated while suppressing 80% of the H_2 yield.[33]

Conclusions

These studies on the kinetics of the reaction between iron-activated magnesium particles and water demonstrate that short-lived, partially, and fully solvated electrons (e_p^- and e_s^-) are precursors of dihydrogen, and that they and hydrogen atoms ($H^\bullet$) formed from them can be scavenged, resulting in suppressed H_2 yields. In the absence of scavengers, e_s^- and $H^\bullet$ each react bimolecularly to give dihydrogen. Consequently, it is possible and practical to choose solutes with suitable solubilities and with appropriate rate constants for reaction with e_p^-, e_s^-, or $H^\bullet$ to suppress H_2 formation, while otherwise controlling the overall rate of reaction of iron-activated magnesium with water by adjusting $[Cl^-]$ or pH. The model developed herein provides a better understanding of the many roles played by magnesium in technology, especially with regard to corrosion, and the formulation of chemical heaters and underwater H_2-generators.

Acknowledgment. We thank Donald Pickard for his interest in and support of this project, and Edward W. Ross for his help in developing mathematically sound techniques for the extraction of reliable rate data from calorimetric measurements.

References and Notes

(1) Raynor, G. V. *The Physical Metallurgy of Magnesium and Its Alloys*; Pergamon Press: New York, 1959.
(2) Cotton, F. A.; Wilkinson, G. *Advanced Inorganic Chemistry, 5th ed.*; John Wiley & Sons: New York, 1988.
(3) Perrault, G. G. In *Encyclopedia of Electrochemistry of the Elements*; Bard, A. J., Ed.; Marcel Dekker: New York and Basel, 1978; Vol. VIII, pp 263–319.
(4) Topper, H. H. *Educ. Chem.* **1978**, *15*, 134.
(5) Folomeev, A. I. *Zh. Prikl. Khim.* **1986**, *59*, 267–270.
(6) Kuhn, W. E.; Friedman, I. L.; Summers, W.; Szegvari, A. In *ASM Handbook Vol. 7: Powder Metallurgy*; ASM International: Materials Park, OH, 1984; pp 56–70.
(7) Kustin, K.; Ross, E. W. *J. Chem. Educ.* **1993**, *70*, 454–459.
(8) Feigl, F.; Anger, V.; Oesper, R. E. *Spot Tests in Inorganic Analysis*, Sixth English Edition; Elsevier Publishing Company: Amsterdam, 1972.
(9) Makar, G. L.; Kruger, L. *Int Mater Rev* **1993**, *38*, 138–153.
(10) Weisz, P. B.; Goodwin, R. B. *J. Catal.* **1966**, *6*, 227–236.
(11) Jordan, P. C. *Chemical Kinetics and Transport*; Plenum Press: New York, 1979.
(12) Ross, A. B.; Mallard, W. G.; Helman, W. P.; Buxton, G. V.; Huie, R. E.; Neta, P. *NDRL-NIST Solution Kinetics Database:-Ver. 3.0*; Notre Dame Radiation Laboratory, Notre Dame, IN, and National Institute of Standards and Technology, Gaithersburg, MD 1998.
(13) Hunt, J. W. In *Advances in Radiation Chemistry*; Burton, M., Magee, J. L., Eds.; John Wiley: New York, 1976; Vol. V, pp 185–315.
(14) Jonah, C. D.; Miller, J. R.; Matheson, M. S. *J. Phys. Chem.* **1977**, *81*, 1618–1622.
(15) Balkas, T. I.; Fendler, J. H.; Schuler, R. H. *J. Phys. Chem.* **1970**, *74*, 4497–4505.
(16) Pimblott, S. M.; LaVerne, J. A. *J. Phys. Chem. A* **1998**, *102*, 2967–2975.
(17) *MATLAB*; The MathWorks, Inc., 24 Prime Park Way, Natick, MA 01760, 508 647 7000.
(18) Tomashov, N. D. *Theory of Corrosion and Protection of Metals*; The MacMillan Company: New York, 1966.
(19) Duplâtre, G.; Jonah, C. D. *Radiat. Phys. Chem.* **1985**, *24*, 557–565.
(20) Steen, H. B. *J. Phys. Chem.* **1970**, *74*, 4059–4061.
(21) Hughes, G.; Roach, R. J. *Chem. Commun.* **1965**, 600–601.
(22) Walker, D. C. *Can. J. Chem.* **1966**, *44*, 2226–2229.
(23) Walker, D. C. *Can. J. Chem.* **1967**, *45*, 807–811.
(24) Sternberg, H. W.; Markby, R. E.; Wender, I.; Mohilner, D. M. *J. Am. Chem. Soc.* **1967**, *89*, 186–187.
(25) Gillis, H. A.; Quickenden, T. I. *Can. J. Chem.* **2001**, *79*, 80–93.
(26) Gauduel, Y.; Pommeret, S.; Migus, A.; Antonelli, A. *J. Phys. Chem.* **1989**, *93*, 3880–3882.
(27) Pépin, C.; Goulet, T.; Houdet, D.; Jay-Gerin, G.-P. *J. Phys. Chem. A* **1997**, *101*, 4351–4360.
(28) Goulet, T.; Pépin, C.; Houdet, T.; Jay-Gerin, G.-P. *Radiat. Phys. Chem.* **1999**, *54*, 441–448.
(29) Kimura, Y.; Alfano, J. C.; Walhout, P. K.; Barbara, P. F. *J. Phys. Chem.* **1994**, *98*, 3450–3458.
(30) Pastina, B.; LaVerne, J. A.; Pimblott, S. M. *J. Phys. Chem. A* **1999**, *103*, 5841–5846.
(31) La Verne, J. A.; Pimblott, S. M. *J. Phys. Chem. A* **2000**, *104*, 9820–9822.
(32) Konovalov, V. V.; Raitsimring, A. M.; Tsvetkov, Yu. D. *Radiat. Phys. Chem.* **1988**, *32*, 623–632.
(33) Taub, I. A.; Kustin, K. U.S. Patent 5,517,981, May 21, 1996.